Preparation for and performance of a *Pseudomonas aeruginosa* biofilm experiment on board the International Space Station

Pamela Flores [a], Rylee Schauer [a], Samantha A. McBride [b,c], Jiaqi Luo [d], Carla Hoehn [a],
Shankini Doraisingam [a], Dean Widhalm [a], Jasmin Chadha [a], Leah Selman [a],
Daniel Wyn Mueller [d], Shannon Floyd [a], Mark Rupert [a], Sridahr Gorti [e], Shawn Reagan [e],
Kripa K. Varanasi [b], Christina Koch [f], Jessica U. Meir [f], Frank Muecklich [d], Ralf Moeller [g],
Louis Stodieck [a], Stefanie Countryman [a], Luis Zea [a,*]

[a] *BioServe Space Technologies, University of Colorado Boulder, 3775 Discovery Drive, Boulder, CO, 80303, USA*
[b] *Massachusetts Institute of Technology (MIT), 77 Massachusetts Ave, Cambridge, MA, 02139, USA*
[c] *Princeton University, Princeton, NJ, 08544, USA*
[d] *Saarland University, 66123, Saarbrücken, Saarland, Germany*
[e] *NASA Marshall Space Flight Center, Martin Rd SW, Huntsville, AL, 35808, USA*
[f] *NASA, Johnson Space Center, 2101 E NASA Pkwy, Houston, TX, 77058, USA*
[g] *German Aerospace Center (DLR), Cologne, Germany*

ARTICLE INFO

ABSTRACT

Biofilms are problematic on Earth due to their ability to both degrade the materials upon which they grow and promote infections. Remarkably, 65% of infections and 80% of chronic diseases on Earth are associated with biofilms. The impact of biofilms is even greater in space, as the crew's lives and mission success depend on nominal operation of mechanical systems which can be interrupted by material damage associated with biofilm growth. Furthermore, the isolated confined environment nature of spaceflight may increase the rates of disease transmission. In the case of the International Space Station (ISS), biofilms are an identified problem on the Environmental Control and Life Support System (ECLSS), namely on the water processor assembly (WPA). In late 2019, the bacterial component of the Space Biofilms experiment launched to ISS to (*i*) characterize the mass, thickness, morphology, and gene expression of biofilms formed in space compared to matched Earth controls, (*ii*) interrogate the expression of antimicrobial resistance genes, and (*iii*) test novel materials as potential biofilm control strategies for future ECLSS components. For this, 288 bacterial samples were prepared prior to the launch of the Northrop Grumman CRS-12 mission from NASA's Wallops Flight Facility. The samples were integrated into the spaceflight hardware, BioServe's Fluid Processing Apparatus (FPA), packed in sets of eight in Group Activation Packs (GAP). Half of these samples were activated and terminated on orbit by NASA astronauts Jessica Meir and Christina Koch, while the remaining half were processed equivalently on Earth. The spaceflight bacterial samples of Space Biofilms returned on board the SpaceX CRS-19 Dragon spacecraft in early 2020. We here describe the test campaign implemented to verify the experiment design and confirm it would enable us to achieve the project's scientific goals. This campaign ended with the Experiment Verification Test (EVT), from which we present example morphology and transcriptomic results. We describe in detail the sample preparation prior to flight, including cleaning and sterilization of the coupons of six materials (SS316, passivated-SS316, lubricant impregnated surface, catheter-grade silicone with and without a microtopography, and cellulose membrane), loading and integration of growth media, bacterial inoculum, and the fixative and preservative to enable experiment termination on orbit. Additionally, we describe the performance of the experiment on board

the ISS, including crew activities, use of assets, temperature profile, and experiment timeline; all leading to a successful spaceflight experiment. Hence, this manuscript focuses on the steps implemented to ensure the experiment would be ready for spaceflight, as well as ISS and ground operations, with results presented elsewhere. The processes discussed here may serve as a guideline to teams planning their own gravitational microbiology experiments. This material is based upon work supported by the National Aeronautics and Space Administration under Grant No. 80NSSC17K0036.

Acronyms/abbreviations

COTS	Commercial Off-The-Shelf
ConOps	Concept of operations
DAPI	4,6-diamidino-2-phenylindole nucleic acid stain
DI	deionized
DLIP	Direct Laser Interference Patterning
DOE	diffractive optical element
ECLSS	Environmental Control and Life Support System
EM	Extracellular Matrix
EVMS	Eastern Virginia Medical School
EVT	Experiment Verification Test
FEP	Fluorinated Ethylene Propylene
FPA	Fluid Processing Apparatus
GAP	Group Activation Packs
ICE	Isolated Confined Environment
ISS	International Space Station
LBG	LB broth (Lennox) supplemented with Glucose
LBK	LB broth (Lennox) supplemented with KNO_3
LIS	Lubricant Impregnated Surface
mAUMg-hi Pi	modified Artificial Urine Media supplemented with glucose and high phosphate
PA14	*P. aeruginosa* UCBPP-PA14 strain
PBS	Phosphate Buffered Saline
PFA	Paraformaldehyde
PI	Propidium Iodide
pSS316	passivated Stainless Steel 316
RIN	RNA Integrity Number
SABL	Space Automated Bioproduct Lab
SS316	Stainless Steel 316
UTIs	Urinary Tract Infections
WPA	Water Processor Assembly

---

1. Introduction

Bacterial biofilms are communities of bacterial cells tightly attached to each other and to other surfaces in a self-produced extracellular matrix (EM) [1] that provides them with protection from disinfectants, antibiotics, and environmental conditions [2]. Biofilms represent a risk to hardware due to their ability to deteriorate and corrode the materials upon which they grow [3], which could result in system malfunction. More importantly, biofilms pose a critical health risk due to their increased resistance to antibiotics [4], which could contribute to recurrent infections. On Earth, 65% and 80% of infections and chronic diseases are associated with biofilms, respectively [5].

In space, biofilms represent a risk because the mission success depends on nominal operation of all mechanical systems. Biofilms found in the Soviet/Russian Mir Space Station were reported as a risk for materials in contact with water and air [6]. Risk for material components can have higher consequences if life supporting functions, such as those performed by the Environmental Control and Life Support System (ECLSS) are impacted. The International Space Station's (ISS) ECLSS has highlighted this risk, as biofilms have been found to have grown inside the Water Processing Assembly (WPA) [7–9]. Biofilm growth within the ECLSS has previously led to filter clogging and loss of operational efficiency [7].

Isolated confined environments (ICE) can increase the risk of certain gastrointestinal and respiratory infections [10], highlighting the health risk that biofilm infections pose in the ICE of spacecraft, including the ISS, other stations, and spacecraft for future missions to Lunar orbit, Mars, and beyond [11]. Urinary tract infections (UTIs) are particularly problematic since they are one of the most common community infections [12]. Recurrent UTIs are highly associated with biofilm formation and antibiotic resistance [4,13]. If left uncleared, a UTI can cause permanent kidney damage, renal failure, urethral narrowing, and sepsis [14]. According to NASA's Integrated Medical Model, urosepsis is considered the third most likely reason for emergent medical evacuation from the ISS [15].

To study the effect of microgravity on biofilm formation, the Space

Biofilms experiment included samples of *Pseudomonas aeruginosa*, the second most common causative agent of UTIs on Earth [16]. The bacterial component of the Space Biofilms experiment was sent to the ISS in late 2019. The project's goals were to (*i*) characterize the mass, thickness, morphology, and gene expression of biofilms formed in space with respect to matched Earth controls, (*ii*) interrogate the expression of antimicrobial resistance genes, and (*iii*) test novel materials as potential biofilm control strategies for future ECLSS components. Here, we present the key steps of the experiment design maturation (Section 2) that culminated with the experiment verification test (EVT) (Section 3), which led to the approval-for-flight of the experiment. We also describe the preparation of the spaceflight experiment prior to launch (Section 4) and the performance of both space and ground operations (section 5).

2. Experiment design maturation

P. aeruginosa UCBPP-PA14 strain (PA14) was selected due to its relevance as a biofilm model organism and as an opportunistic pathogen [17]. The first aspect tested was the growth dynamics of PA14 in commercial off-the-shelf (COTS) microplates using different culture media under aerobic conditions. The growth was tested using six different media and it was determined that LB Broth (Lennox) supplemented with glucose (LBG) was best at enabling bacterial growth (data not shown).

After confirming growth in COTS microplates at 37 °C in aerobic LBG, the compatibility of these growth conditions in spaceflight hardware (BioServe Space Technologies' 12-Well BioCell) was assessed. Initially, planktonic growth was achieved in BioServe's 12-Well BioCell using LBG. However, *P. aeruginosa* tended to prefer forming biofilms on the gas-permeable Fluorinated Ethylene Propylene (FEP) membranes of the BioCell, rather than on the material surfaces being tested (aluminum, cellulose membrane, and lubricant impregnated surface [LIS]). Additionally, the oxygen availability inside the BioCell was limited in comparison to the COTS well plates, creating a semi-anaerobic (hypoxic) environment. The flight hardware was therefore changed to BioServe's Fluid Processing Apparatus (FPA) – which has been previously operated in space over 5,000 times – to avoid a hypoxic environment and to ensure strict anaerobic conditions, similar to what is experienced in the WPA where biofilms have been observed. To sustain

PA14's growth in anaerobic conditions, potassium nitrate (0.86% m/v) was added to the LB Lennox media (LBK) as a terminal electron acceptor and the glucose supplement was removed. Growth dynamics were tested once more using LBK at 37 °C in anaerobic conditions in the FPAs and successful planktonic growth and biofilm formation was achieved on all material surfaces (see Appendix A).

The material surfaces to be tested were determined based on their spaceflight and medical relevance as described in Zea et al. (2018) [8]. The chosen materials were Stainless Steel 316 (SS316) due to its application in spacecraft tanks and tubes, and especially due to its use in the waste water tank of the WPA; passivated SS316 (pSS316) due to its use in the ECLSS potable water tank and tubes; the novel LIS (lubricant impregnated surface) made out of a silica wafer impregnated with silicone oil as a potential biofilm-inhibiting substitute for SS316 [18]; cellulose membrane to replicate previous flight studies that found a column-and-canopy structure of *P. aeruginosa* biofilms grown in spaceflight [19], catheter-grade silicone due to its implication as risk factor to develop UTIs, and catheter-grade silicone with ultrashort-pulsed direct laser interference patterning (DLIP) [20] as a potential biofilm-control topography strategy for catheters and other surfaces. Each material was cut into 1 cm^2 coupons that fit in the FPA. LBK simulated nutrient-rich wastewater and was used as media for SS316, pSS316, and LIS. To interrogate the column-and-canopy structure reported previously, and because catheters are in contact with urine, modified Artificial Urine Media supplemented with glucose and high phosphate (mAUMg-hi Pi) [19] was chosen for cellulose, silicone, and silicone DLIP.

The compatibility of mAUMg-hi Pi with PA14 with the FPAs was tested, and successful planktonic growth and biofilm formation on the material coupons was confirmed (see Appendix A). With this, the focus turned to hardware-associated testing. On the material side, it was confirmed that the silicone oil of LIS was not bactericidal (see Appendix

B). On the hardware side, it was decided to use the FPA in a three-chamber configuration (see Fig. 1 showing how the media, bacteria in stasis, and fixative/preservative were separated) to be able to launch the experiment inactivated for activation on orbit (to allow biofilm formation) and termination in the microgravity environment on the ISS. The three chambers were arranged as follows: chamber A (see Fig. 1) filled with sterile growth media and containing a material coupon; chamber B filled with bacterial inoculum in stasis (suspended in phosphate buffered saline [PBS] without any carbon source); and chamber C with paraformaldehyde (PFA) as fixative (for post-flight phenotypic analyses) or RNAlater as preservative (for transcriptomics), depending on the sample. A double-sided tape was used to immobilize the material coupon in chamber A. The tape was also tested for biocompatibility and exhibited no interference in bacterial growth or biofilm formation.

To keep the samples contained and to allow for simultaneous activation/termination, eight FPAs were assembled in BioServe's Group Activation Pack (GAP). The plan for spaceflight was that the integrated FPA/GAPs were to be sent at 4 °C to the ISS and, once there, activation would occur by mixing chambers A and B followed by incubation at 37 °C to elicit biofilm formation. Termination would be performed in space by mixing in the contents of chamber C. After termination, samples were to be stowed at 4 °C (fixed samples) or −80 °C (preserved samples) until return to Earth.

Additional tests were conducted to ensure the experiment design would enable realization of the project's goals. Since RNA sequencing requires well-preserved RNA, we tested the biofilm RNA quality as a function of incubation days (see Fig. 2). The quality of RNA, quantified using the RNA Integrity Number (RIN), decreased after three days of incubation past the minimum needed for RNA sequencing (RIN = 5). Such decrease correlates with the decline in viability of the biofilm cells (see Fig. 3), as RNA degrades rapidly in non-viable cells [21,22]. Hence the experimental time points were set to 1, 2, and 3 days of incubation. Fig. 3, shows differences in biofilm viability in time based on the surface material and media. For SS316 in LBK, viability increases from day 1 to day 2 and then starts progressively declining. The increase in viable cell count could be attributed to the growth of the biofilm over the material surface, both in surface area covered with biofilm as well as robustness of the biofilm; while the decrease in viable cells could be interpreted as the decay of cells in the biofilm due to depletion of nutrients in the media. For silicone in mAUMg-hi Pi, there is a drop in viability on day 2
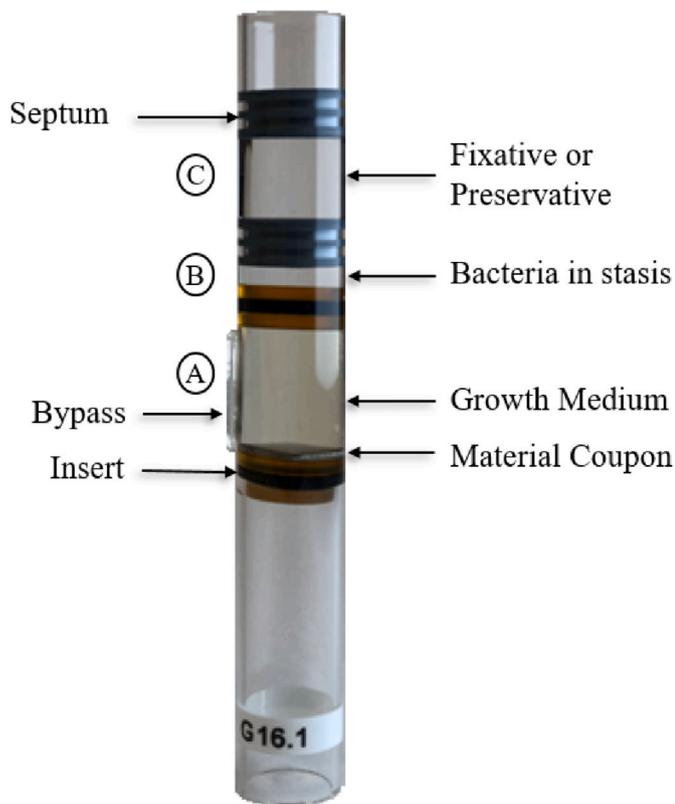

Fig. 1. BioServe Space Technologies' Fluid Processing Apparatus (FPA) in a three-chamber (A–C) configuration as used in the Space Biofilms bacterial experiment.
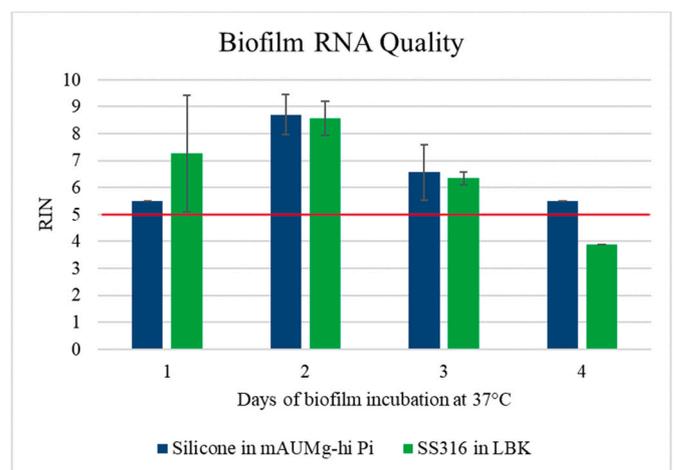

Fig. 2. Biofilm RNA quality per incubation time. Red line marks the ideal minimum quality needed for RNAseq. RIN = RNA Integrity Number. Error bars represent 95% confidence interval. N = 3 biological replicates, except for silicone day 1 (N = 1), SS316 day 2 (N = 2), day 4 (N = 1) because RNA was degraded and the RIN could not be calculated by software. Data obtained from multiple experiments. (For interpretation of the references to color in this figure legend, the reader is referred to the Web version of this article.)
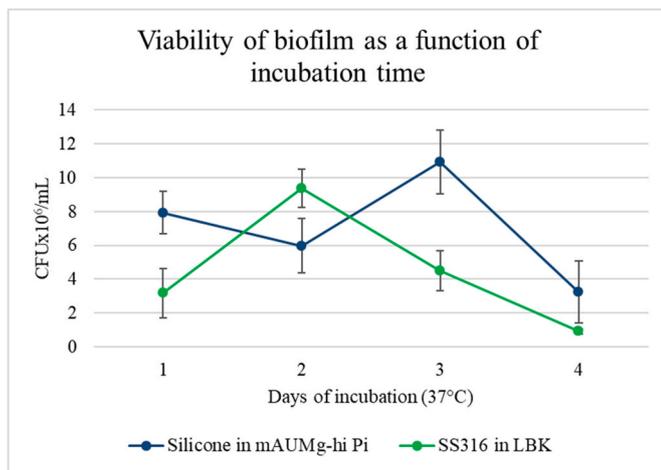
Viability of biofilm as a function of incubation time

Fig. 3. Viability of biofilm cells per incubation time. CFU = Colony Forming Units. Error bars represent 95% confidence interval. N = 3 biological replicates each with CFU counts on 3 dilution plates.

that might indicate biofilm detachment events [23] or cell differentiation through directed cell death [24].

After 24 h of incubation, PA14 produced enough gas to push the inserts and increase the chamber volume, with LBK having more gas production than mAUMg-hi Pi. LBK produced a maximum of 1.72 cm of displacement after 72 h of incubation (see Appendix C). Using a 2.25 safety factor, a maximum displacement of ~4 cm of uncompressed gas and ~1 cm of compressed gas was estimated. In order to leave space for gas expansion and avoid pressurization, the chamber volumes were set to: 2.75 ml of media, 0.5 ml of inoculum, and 1.75 ml of fixative/preservative in chambers A, B, and C, respectively (see Fig. 1). These volumes were calculated considering the height of two inserts, two septa, and the GAP plunger. Having 1.75 ml in chamber C translated into an RNAlater:liquid culture ratio of 1:2. This ratio was demonstrated to be successful in preserving the nucleic acids in the sample (see Appendix D). For a final fixing concentration of 4% PFA, the fixative was loaded at a concentration of 11.4% PFA in chamber C. Similarly, chamber A was loaded with growth media at a 1.18x concentration, so that after mixing with Chamber B, a 1x concentration would be achieved.

To characterize the morphology of the biofilms, Z-stacks of images were acquired using fluorescent confocal microscopy of the PFA samples. The staining protocol was standardized by trying different nucleic, lipid, and saccharide stains. Based on biofilm penetration, signal bleed-through between fluorescent channels, and sharpness of the staining, FilmTracer FM 1–43 Green Biofilm (Invitrogen, Cat. F10317) (to stain lipids, cell membranes in particular) and Propidium Iodide (PI) (PromoKine, Cat. PK-CA707-40017) (to stain nucleic acids) were chosen. Z-stacks of the biofilms were captured and visualized in Nikon's NIS-Elements Viewer as 3D images, and were analyzed in COMSTAT2 to quantify factors as biomass, thickness, roughness, and percent of surface covered by biofilm.

To elucidate the gene expression of the biofilms, the RNAlater samples were processed for RNA-seq. This data was used for whole transcriptome differential expression analysis. The protocol of RNA extraction was tested using samples of biofilms grown over material coupons, and all samples yielded sufficient RNA of excellent quality (RIN ≥ 5 and mass ≥ 100 pg) for sequencing with Illumina using the SMARTer® Stranded Total RNA-Seq Kit v3 -Pico Input (Takara, Cat. 634,485) library preparation kit. Since our interest was analyzing the transcriptome of the biofilm, it was important to confirm that the collected samples had no planktonic-cell RNA (henceforth referred to as RNA contamination). To do this, after biofilm formation, the liquid culture of some samples was switched with *Escherichia coli* liquid culture of the same concentration. Then biofilm samples were prepared for RNA

extraction (as planned for post-flight), but instead of extracting RNA, samples were used to run PCR tests with two sets of primers specific for *E. coli* (targeting either *uspA* or *uidA* genes) (see Table 1). The absence of any amplification confirmed that the biofilm samples had no planktonic contamination (see Appendix E).

A crucial constraint to consider in space science is the period of time between when samples are prepared and handed over to NASA prior to launch, and when the experiment is started on orbit. In this experiment, the loaded FPAs were stored at 4 °C during this period of time. To ensure experiment success, the viability of bacteria and media in cold stowage (4 °C) was tested. PA14 cells remained 88–99% viable for 20 days stored at 4 °C (see Appendix F), while media could be stored at 4 °C for up to 6 months without compromising bacterial growth (see Appendix G). Urea in the mAUMg-hi Pi media was also found to be stable for at least 20 days during 4 °C storage (see Fig. 4). Hence, a limit of 20 days from experiment assembly to activation was required to guarantee correct preservation of all biological components.

The post-ops cold stowage – the time between sample fixation/preservation on orbit and when our team would receive it back in our lab for analyses – was also tested using samples that were terminated and cold stowed for 64 days at 4 °C (PFA) or −80 °C (RNAlater). This simulated the time that samples would spend on orbit before they got back to Earth. Results showed no impact on the samples and confirmed the possibility of obtaining data for morphology and RNA extraction (see Appendix H). This concluded the tests and standardization before the experiment verification test (EVT), having optimized all procedures from experiment assembly to data acquisition.

3. EVT results

For the EVT, the same procedures as those described in Sections 4 and 5 were followed, with the exception of having three replicates per condition instead of four, and the experiment taking place in our lab instead of on ISS. Nevertheless, the same timeline, hardware, and protocols designed for spaceflight operations were implemented on the EVT. After experiment operations, samples were taken out of cold stowage and FPAs disassembled from the GAPs. Coupons were recovered from the FPAs using a Lexan rod to push from chamber C side upwards, first exposing the coupon by the edge of the FPA and subsequently allowing us to aspirate the liquid culture. Each coupon was gently detached from the insert by grabbing it with tweezers by the sides and placed facing up in a well of a COTS 24-well plate. The coupon with the biofilm was gently washed three times with 1 ml PBS to get rid of any remaining planktonic cells, and then further processed (described below) for either microscopy or transcriptomic analyses. The planktonic cell culture was homogenized by pipetting up and down and then it was either refrigerated at 4 °C or cryopreserved at −80 °C for PFA or RNAlater samples, respectively.

3.1. Morphology analysis

For PFA samples, once the coupon was washed with PBS, the biofilm was stained with 4,6-diamidino-2-phenylindole (DAPI) (1 μg/ml) for 10 min and then with FilmTracer 1–43 Green Biofilm (10 μg/ml) for 30 min. For the EVT, DAPI was used instead of PI, because at this point the use of PI had not been tested. However, the results from the EVT showed that some images had less-than-ideal penetration of the stain, which led

Table 1
uspA and *uidA* primer information (adapted from Ref. [25]).

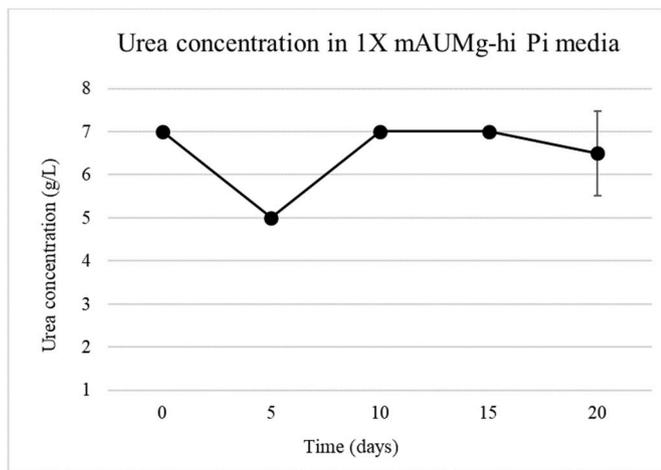| ID	Sequence	Fragment size	Ref.
uspA F	5′ ccgatacgctgccaatcagt 3′	884bp	Chen and Griffiths [26]
uspA R	5′ acgcagaccgtaggccagat 3′		
uidA F	5′ tatggaatttcgccgatttt 3′	166bp	Heijnen and Medema
uidA R	5′ tgtttgcctccctgctgcgg 3′		[27]

Fig. 4. Stability of urea in mAUMg-hi Pi at 4 °C over time. Error bars represent 95% confidence interval. N = 2 replicates.

to testing PI as an alternative. Changes to protocol are strongly discouraged after an experiment's EVT, but in this case, the switch to PI was proven to be necessary. PI produced better results than DAPI in that the shape of a cell was clearer and the fluorophore brightness was increased and more uniform across samples. Those improvements allowed the use of the images without performing any brightness and contrast adjustments (which were needed with DAPI) such that the analysis was more impartial and less user-dependent.

Stained samples were mounted onto glass slides using gorilla glue and topped with VectaShield (Vector Laboratories, Cat. H-1400-10) and a coverslip. 3D imaging was done at 100X in a Nikon SIM/A1 Laser scanning Confocal Microscope. Image acquisition was performed on two fields of view (125×125 μm) per coupon. For flight samples, four fields of view on the center of the coupon were acquired instead of two. The resulting nd2 files were visualized as 3D images using Nikon's NIS- Elements Viewer (see Fig. 5). The nd2 files were also transformed to tiff files using ImageJ and both fluorescent channels used to quantify biomass ($\mu m^3/\mu m^2$), and thickness (μm) in COMSTAT2 (see Fig. 6). Obtaining these results confirmed that the post-flight microscopy protocol would achieve qualitative and quantitative morphology analysis of the biofilms.

Images of the biofilms grown on all material surfaces were acquired. The 3D volume view provided a visual representation of the biofilm morphology and showed changes in biofilm formation by incubation time and by material surface (see Fig. 5). For the EVT (as for flight

samples), the biomass and thickness of the biofilms were measured using the publicly available software COMSTAT2. The results in Fig. 6 confirmed that the protocol was sensitive enough to detect significant differences.

3.2. Transcriptomic analysis

For RNAlater samples, once the coupon was washed with PBS, the PBS was discarded and 1 ml of fresh RNAlater was added to each well. The plate was sealed with an RNAse/DNAse free (Sigma, Cat. T9696-100 EA) membrane and sonicated at 40 kHz for 15 min at room temperature to detach the biofilm from the coupon. The RNAlater with the suspended biofilm was used to extract RNA with the Zymo Research Quick-RNA Fungal/Bacterial microprep Kit (Cat. R2010). Quality, through RNA Integrity Number (RIN), and quantity of the extracted RNA was assessed through BioAnalyzer (B) and/or TapeStation (T) (see Table 2).

The EVT quality and quantity results showed that 72% of samples yielded excellent RNA (RIN ≥5 and mass ≥100 pg), 8% good RNA (RIN ≥4 and mass ≥20 pg, colored green), 6% poor RNA (RIN ≥3 and mass ≥10 pg, colored yellow), and 14% failure (RIN < 3 and mass < 10 pg, colored red). These results showed unsuccessful RNA extraction for both of the silicone materials. Since the biofilm detachment procedure was done with sonication, it was hypothesised that the more-flexible silicone material absorbed some vibration, potentially hindering biofilm detachment. A solution was established by adding an extra step of vortexing to increase the amount of RNA extracted from silicone samples (data not shown).

4. Spaceflight experiment preparation

The following describes the steps performed to prepare the 144 flight and 144 ground samples of the Space Biofilms bacterial experiment, which took place at the Eastern Virginia Medical School (EMVS) unless otherwise indicated. The experiment independent variables were gravitational regime (Earth gravity and microgravity), incubation times (1, 2, and 3 days), material-media combinations (LBK for SS316, pSS316, and LIS; mAUMg-hi Pi for cellulose, silicone, and silicone DLIP), fixative/preservative (PFA and RNAlater), and replicates (four).

4.1. Hardware preparation

LIS coupons were prepared at the Massachusetts Institute of Technology under sterile conditions by first etching nano-scale roughness onto silica wafers using reactive ion etch. Then, silica wafers were thoroughly cleaned in a bath of deionized (DI) water and detergent and
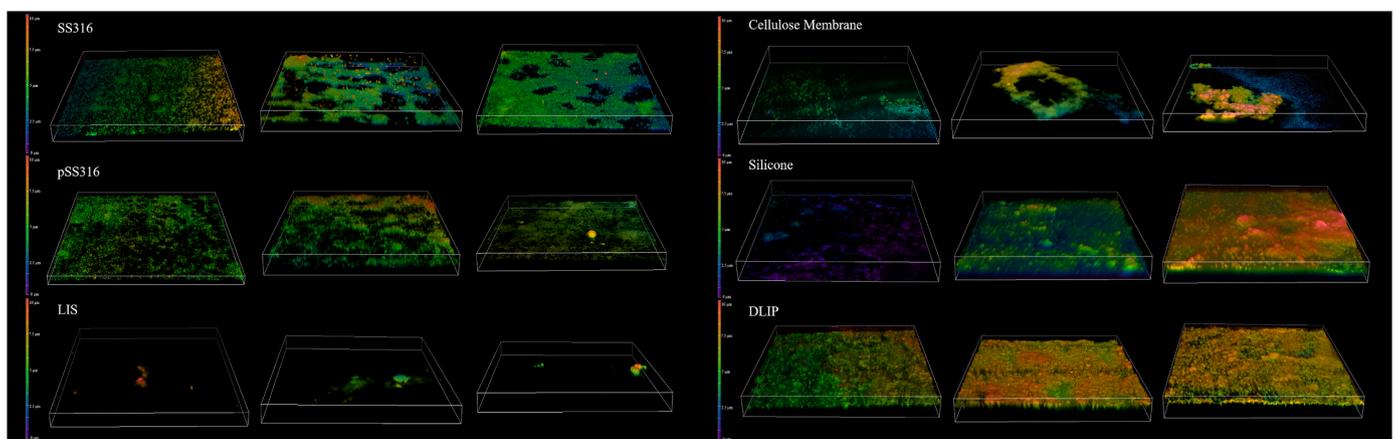

Fig. 5. 3D structure of PA14 biofilm by material and incubation time. Images were generated by Nikon's NIS-Element Viewer and thickness in μm is color-coded. (For interpretation of the references to color in this figure legend, the reader is referred to the Web version of this article.)
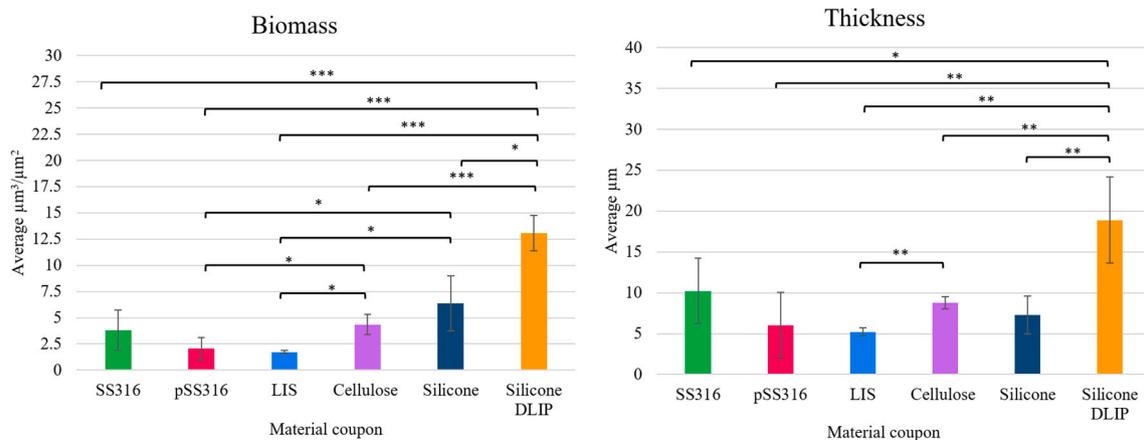
Fig. 6. Biomass and thickness of PA14 biofilms formed over different material surfaces at 1 day of incubation. Error bars represent 95% confidence interval. Significant differences with p-value *<0.05 ** < 0.01 ***<0.001. N = 3 coupons with 2 fields of view imaged per coupon.

Table 2
Quality (RIN values) and quantity (mass) results for the RNA extracted from the EVT biofilm samples. Color code: white is excellent (RIN ≥5 and mass ≥100 pg), green is good (RIN ≥4 and mass ≥20 pg), yellow is poor (RIN ≥3 and mass ≥10 pg), and red is failure (RIN <3 and mass <10 pg).

Material	Day 1		Day 2		Day 3	
	RIN (T/B)	Mass (pg)	RIN (B)	Mass (pg)	RIN (B)	Mass (pg)
SS316	9.4/5.6	1924	8.4	2780	7.7	6112
	10/6.7	1280	4.8	572	6.2	9388
	10/4.5	1352	4.6	1520	6.5	4332
pSS316	8.6/4.9	1844	8.4	716	6.8	9644
	10/9.3	1536	5.8	892	7.1	3372
	5.3/7.7	1004	8.3	3428	5.9	4616
LIS	9.2/8.9	2844	7.1	1228	7.1	8644
	NA/7.8	116	5.3	2216	7.0	2544
	7.6/NA	352	8.7	2060	7.5	2064
Cellulose	6.6/5.6	796	9.0	1556	3.7	780
	10/8.2	304	9.3	548	3.0	240
	10/7.6	1524	7.6	1164	6.3	192
Silicone	X*	X*	8.6	668	NA*	264
	1.0	272	5.9	704	2.4	176
	5.5	56	6.1	968	2.5	132
Silicone DLIP	NA*	40	7.7	892	3.6	220
	6.8	108	7.4	664	4.0	72
	1.0	40	NA*	156	2.2	124

*X= not done, NA= not able to determine by software

ethanol and dried by air. Ultrashort-pulsed DLIP patterning of the silicone samples was conducted applying two-beam pulsed laser interference utilizing a Ti:Sapphire Spitfire laser system (Spectra Physics) emitting a pulse duration of 100 fs (full width at half maximum) at a centered wavelength of 800 nm. In the optical DLIP setup, the diameter and polarization of the seed beam is modulated before it gets split into two partial beams by a diffractive optical element (DOE). The partial beams are then focused on the sample's surface by a lens system, where line-like patterns are created by two-beam interference (see Fig. 7) [20]. By aligning the incident angle θ between the two partial beams according to Eq. (1), a periodicity of 3 μm was generated on the silicone samples. Planar patterning was performed by scanning the substrate surface in continuous pulsing mode (pulse frequency 1 kHz, fluence 0.8 J/cm², pulse overlap 57%).
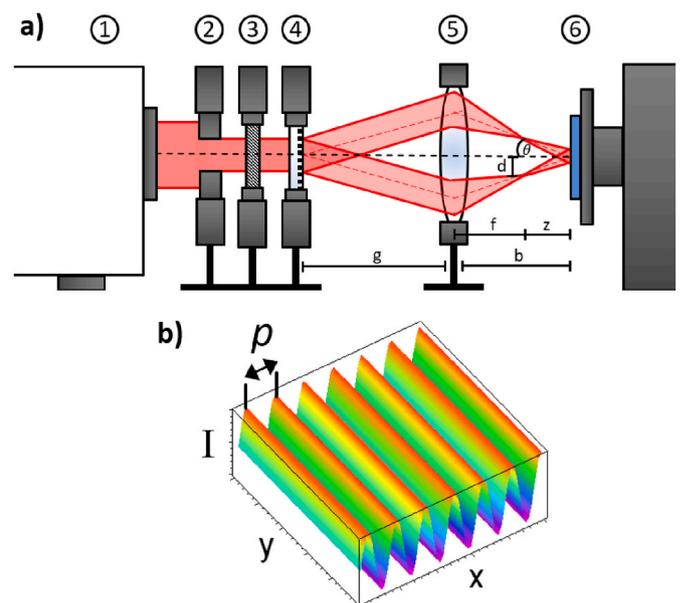
$$P = \frac{\lambda}{2\tan(\theta)} \tag{1}$$

Fig. 7. a) schematic illustration of the optical setup for ultrashort-pulsed DLIP. 1 laser source, 2 aperture, 3 wave plate, 4 DOE, 5 lens system, 6 automated two axes (x, y) sample mount. b) Two beam interference leading to one-dimensional sinusoidal intensity patterns. Periodicity accounts for the distance between two intensity maxima. Adapted with permission from Ref. [20]. Copyright (2020) Springer Nature.

then rinsed with DI water, acetone, and isopropyl alcohol. Once clean, the nano-textured wafers were plasma cleaned to remove any residual organic contamination and to prepare them for functionalization by flourosilane. Flourosilane (1H,1H,2H,2H-perfluorodecyltriethoxy silane) was vapor deposited onto wafers over a period of 6 h to render the material superhydrophobic. Finally, a stable layer liquid was imbued within the superhydrophobic nano-textured wafers by dip-coating the samples into silicone oil and withdrawing at a slow velocity to ensure an even, stable liquid layer.

Silicone DLIP coupons were prepared at Saarland University. Catheter-grade silicone coupons were cleaned in an ultrasonic bath with

The hardware preparation started at BioServe Space Technologies at the University of Colorado Boulder. The glass barrels, O-rings, inserts, rubber septa and coupons (except LIS and cellulose membrane) were cleaned using 1% liquinox (Alconox Inc, Cat. 1201) and thoroughly rinsed with deionized water. Glass barrels were cleaned by hand. O-rings, inserts, rubber septa, silicone and silicone DLIP coupons were bag washed. SS316 coupons were cleaned by ultrasonic bath in liquinox solution (15 min). All hardware and coupons (except LIS and cellulose membrane) were placed in an oven at 100 °C after rinsing until completely dried. LIS coupons were neither cleaned nor dried in this fashion, because they were prepared in sterile conditions. The cellulose membrane coupons were already sterile per manufacturer specifications (MF-Millipore, Cat. GSWP01300).

The glass barrels, rubber septa, and O-rings were submerged in Sigmacote to reduce adhesion of cells (Sigma-Aldrich, Cat. SL2-100 ML) and dried at 100 °C for 30 min. The O-rings were then assembled to the inserts. To prepare the pSS316 coupons, clean SS316 coupons were heated at 82 °C for 120 min in a solution of 4% (w/v) citric acid (Sigma-Aldrich, Cat. C-8385) and then rinsed with deionized water. Coupon size was 1 cm^2, but to facilitate the assembly of the coupons into the FPAs, four or two corners of the coupons were slightly cut for the silicone and LIS, respectively. Cellulose membrane came pre-cut in circles of 1.4 cm diameter that fitted the FPA. The silicone DLIP coupons were cut from a silicone DLIP mat into pieces of 0.635 cm^2 since the material was limited. Coupons and glass barrels were labelled with a unique ID per sample.

Double sided tape (3 M, Cat. 9731) was placed on the entire backside of the coupons and then coupons were installed onto the inserts. The biocompatibility of the two-sided tape was tested and confirmed not to introduce any confounding factors [28]. Immediately, they were matched to their corresponding FPAs and installed. This was done in a way such that the coupons' surface was never touched. Gloves were cleaned with ethanol in between each sample to prevent Sigmacote from the FPAs transferring to the coupons.

4.2. Media preparation

LBK and mAUMg-hi Pi were prepared to a 1.18x concentration to account for the dilution generated by the introduction of the inoculum's liquid volume. 1.18x LBK was prepared dissolving 23.6 g of LB Lennox (Sigma, Cat. L3022), and 10 g of potassium nitrate (Sigma, Cat. P8291) in 1 L of distilled water. 1.18x mAUMg-hi Pi was prepared based on the original 1x recipe of Kim et al. (2013) [19] by dissolving the components listed in Table 3 in 1 L of distilled water (pH 7). Both growth media were filter sterilized with 0.22 μm filters (Nalgene, Cat. 566-0020) and then

Table 3
Components of 1.18x mAUMg-hi Pi medium.

Reactive	Amount	Manufacturer and Catalog number
(L-) Lactic acid	0.098 ml	TCI, L0165
Ammonium chloride	1.320 g	Sigma Aldrich, 254,134
Calcium chloride dihydrate	0.038 g	Fisher, BP510
Creatinine	0.782 g	Alfa Aesar, B23097
Di-potassium hydrogen phosphate	4.941 g	Fisher, P288
Glucose	0.356 g	Fisher D16
Iron II sulphate heptahydrate	0.0012 g	Acros, 423,730,050
L-glutamine 200 nM solution	9.845 ml	Sigma Aldrich, G7513
Magnesium sulphate heptahydrate	0.485 g	LabGuard, 4200
Potassium dihydrogen phosphate	3.862 g	Alfa Aesar, 11,594
RPMI 1640 amino acids 50X solution	19.697 ml	Sigma Aldrich, R7131
Sodium bicarbonate	2.068 g	Sigma Aldrich, S5761
Sodium chloride	5.181 g	Mallinckrodt chemicals, 7581-6
Sodium nitrate	0.504 g	RICCA, RDCS0650
Sodium sulphate decahydrate	3.172 g	Acros, 125,012,500
Urea	10.055 g	Fisher, BP169
Uric acid	0.065 g	Sigma Aldrich, U2625

stored at 4 °C. PBS was prepared per manufacturer instructions (Sigma Aldrich, Cat. P4417) by dissolving one tablet per 200 ml of deionized water to yield a 0.01 M phosphate buffer, 0.0027 M potassium chloride, and 0.137 M sodium chloride solution (pH 7.4), and autoclaved at 121 °C for 30 min. PBS was stored at 4 °C. A new LB agar plate of PA14 (kindly provided by Prof. George O'Toole) was streaked from a cryo-stock and incubated at 37 °C for 24 h. The colonies were inspected to make sure there was nothing unusual about the morphology. Then, LBK medium and mAUMg-hi Pi medium were inoculated with the PA14 and incubated at 37 °C to make sure the prepared media would enable bacterial growth. The bacterial inoculum was prepared from an over-night culture of the PA14 plate. The overnight culture was done by inoculating 6 ml of LBK and incubating at 37 °C for 16 h (OD$_{595}$ 0.706). Then, a 1:100 dilution in PBS was done to make the bacterial inoculum in stasis (OD$_{595}$ 0.001). This inoculum was immediately used to load chamber B (see Section 4.3 for details) in all the flight and ground PFAs (plus spares).

The 11.4% PFA solution was prepared by dissolving 400 ml of 16% PFA (Alfa Aesar, Cat. 43,368) in 160 ml of PBS and stored at 4 °C. The RNAlater (Invitrogen, Cat. AM7021) was poured in 15 ml conical tubes (4 ml per tube) and refrigerated at 4 °C for 3 days. After refrigeration, approximately one out of five tubes had crystals formed. The crystals were pulverized with a homogenizer and then the RNAlater was returned to cold stowage at 4 °C until used to load chamber C.

4.3. Pre-flight science-hardware integration

The FPA glass barrels, inserts (with and without coupons as needed), and the rubber septa were autoclaved at 121 °C for 30 min. Chamber A of the FPAs was loaded with 2.75 ml of either sterile LBK or sterile mAUMg-hi Pi medium. The chamber was closed with an insert making sure no air bubbles were left inside, and the top side of the FPA was covered. A contamination check was done by incubating the FPAs at 37 °C for 24 h. None of the FPAs showed growth of any type, confirming chamber A was loaded without introducing contamination.

The bacterial inoculum in stasis was prepared as described in Section 4.2 and immediately used to load Chamber B with 0.5 ml of it. The chamber was closed with a rubber septum making sure no air bubbles were left inside. Lastly, chamber C was loaded with 1.75 ml of PFA or RNAlater and closed with a rubber septum in the same fashion.

Eight loaded FPAs were integrated into each GAP. The flight and ground GAPs 1–6 contained the samples to be incubated for one day, GAPs 7–12 samples to be incubated for two days, and GAPs 13–18 samples to be incubated for three days. One GAP included a temperature data recorder for each incubation time/gravity condition combination. After integration, all GAPs remained at 4 °C to prevent growth of the bacterial inoculum. The flight GAPs were handed to BioServe for subsequent turnover to NASA in preparation for launch, while ground GAPs were stored at the same temperature (4 °C).

5. Experiment performance

The experiment performance of the flight samples on orbit at the ISS was recorded and the ground samples were operated at BioServe's labs 2 h later – to the minute - to replicate the flight timeline as closely as possible. The following description is based on the flight assets and timeline, but conditions also represent what was done for the ground samples.

The flight operations (see Fig. 8) started on November 2nd, 2019 with samples being launched at 4 °C in Northrop Grumman's CRS-12 mission (NG-12). The Space Biofilms bacterial experiment was performed in space by NASA astronauts Jessica Meir and Christina Koch (see Fig. 9). After berthing, all GAPs were transferred to 4 °C until Nov. 11th when all GAPs were activated in the aisleway of the ISS. Activation was done by attaching a crank to the GAP lid then cranking it to push the system towards the bypass, introducing chamber B fluid into chamber A.
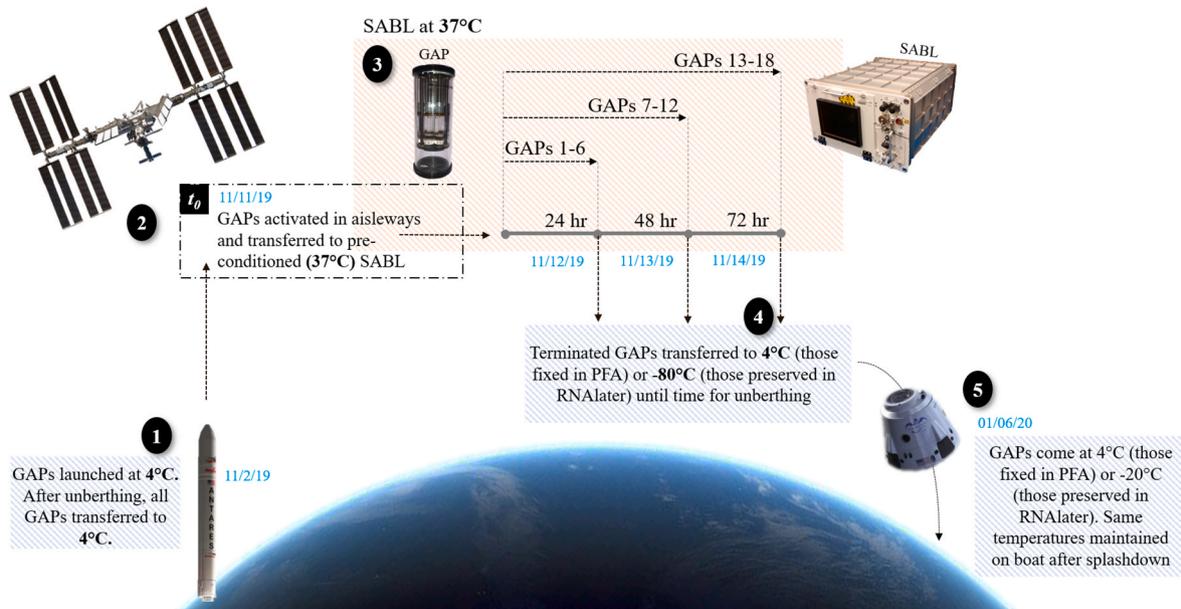
Fig. 8. Concept of operations (ConOps) for the bacterial flight samples of Space Biofilms.

Fig. 9. Astronauts Jessica Meir (top panel) and Christina Koch (bottom panel) cranking BioServe's GAPs to activate and terminate the experiment, respectively, on board the ISS. Credit: NASA.

This placed the bacteria in a nutrient environment where they could grow and form biofilms. To support such growth and biofilm formation, the GAPs were immediately placed at 37 °C in BioServe's Space Automated Bioproduct Lab (SABL) [29] for either 25, 48, or 72 h. After incubation, termination of the experiment was performed on orbit by cranking the GAPs once more to introduce chamber C fluid. This resulted in the fixation with PFA or preservation with RNAlater of the samples. Samples were then transferred to 4 °C or −80 °C cold stow, respectively, until unberthing on January 6th' 2020, when they returned to Earth at 4 °C or −20 °C, respectively, on the SpaceX CRS-19 (SpaceX-19) mission.

The temperature profiles for the activation, incubation and termination of the ground and flight samples were plotted and compared. All samples reached an average incubation temperature of ~38 °C. The mean incubation temperatures for flight/ground samples were 37.0/ 37.8 °C, 37.8/38.0 °C, and 37.7/38.0 °C for one, two, and three days of incubation, respectively. The difference in incubation temperatures between flight and ground samples was in the range of 0.2–0.8 °C, meaning both batches of samples were kept within less than a 1 °C difference.

6. Conclusions and next steps

The Space Biofilms bacterial experiment went through an extensive test campaign of which we here presented the key milestones that helped fine-tune the experimental design, ensuring its readiness for flight. The protocol was tested and confirmed that it would allow for proper data acquisition. Additionally, we confirmed that the operations performed in spaceflight were equivalent to the operations performed on ground, enabling comparisons between conditions that may provide insight into the key differences of biofilm formation in microgravity. Such comparisons and the results from the Space Biofilms bacterial project will be published separately. By exploring the stepwise approach taken to validate our protocols, the contents of this paper may help direct other teams in their efforts of maturing their experimental design and preparing for spaceflight.

Declaration of competing interest

The authors declare the following financial interests/personal relationships which may be considered as potential competing interests: KKV is a co-founder and has an equity interest in LiquiGlide Inc. KKV acknowledges a board position with LiquiGlide Inc.

Acknowledgements

We would like to thank all who have participated and were involved

Appendix A. (PA14 anaerobic growth compatibility test in FPAs)

BioServe's FPAs hardware enabled planktonic growth and biofilm formation in anaerobic conditions. Both LBK and mAUMg-hi Pi liquid cultures of PA14 were visibly turbid after 24 h of incubation at 37 °C (see Fig. 10). PA14 was able to form biofilm on a representative surface for both LBK and mAUMg-hi Pi media. Microscopy images confirmed the presence of the biofilm, and the biomass was calculated (see Fig. 11).

Fig. 10. Anaerobic planktonic growth of PA14 in FPAs. LK are the samples incubated in LBK, while MAUM are the samples incubated in mAUMg-hi Pi. N = 3 replicates.
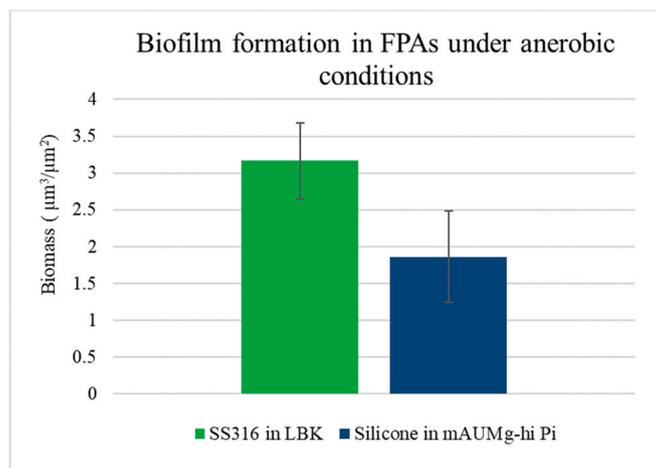

Fig. 11. Biomass of the biofilms formed on SS316 in LBK and on silicone in mAUMg-hi Pi after 48 h of incubation using FPAs. Error bars represent 95% confidence interval. N = 3 biological replicates.

Appendix B. (Lubricant oil bactericidal test)

No difference in bacterial growth was observed *for P. aeruginosa* liquid cultures in contact with LIS's lubricant oil, when compared to growth without lubricant oil (see Fig. 12). This confirms that the lubricant oil used on LIS coupons is not bactericidal, therefore the reduction of biofilm formation observed on this material is not an artifact of the lubricant killing the bacteria.
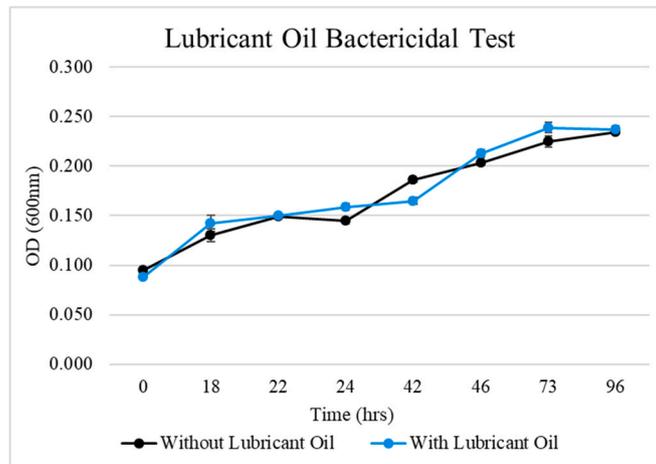

Fig. 12. Lubricant oil bactericidal test, *Pseudomonas aeruginosa* growth curves with or without the addition of LIS's lubricating oil. Error bars represent 95% confidence interval. N = 3 biological replicates.

Appendix C. (PA14 gas production in LBK at 37 °C)

PA14 showed gas production after 24 h of incubation (see Fig. 13). The gas production incremented with time and by 3 days of incubation the gas volume generated a maximum of 1.72 cm of displacement (see Fig. 14). This is enough gas to be able to displace the system and/or pressurize it. This data was taken into consideration when calculating the volumes per chamber, in order to leave the necessary space for displacement in the FPA configuration, so that it would not affect the performance of the experiment.
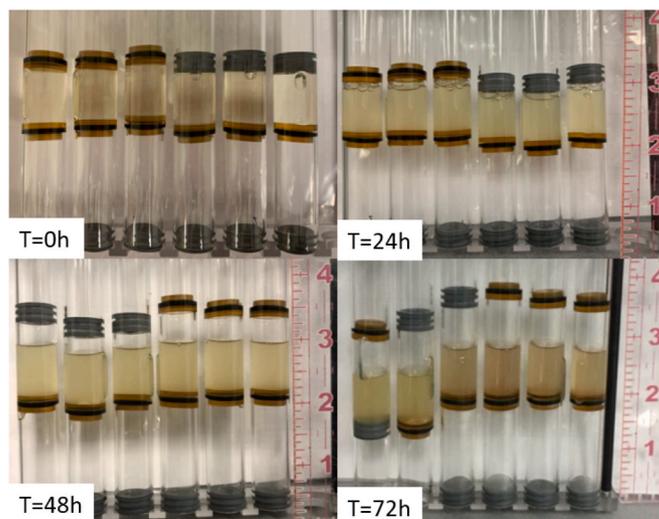

Fig. 13. Gas production of PA14 in LBK by incubation time at 37 °C. Half samples had insert tops and the other half had septa tops. N = 3 biological replicates.
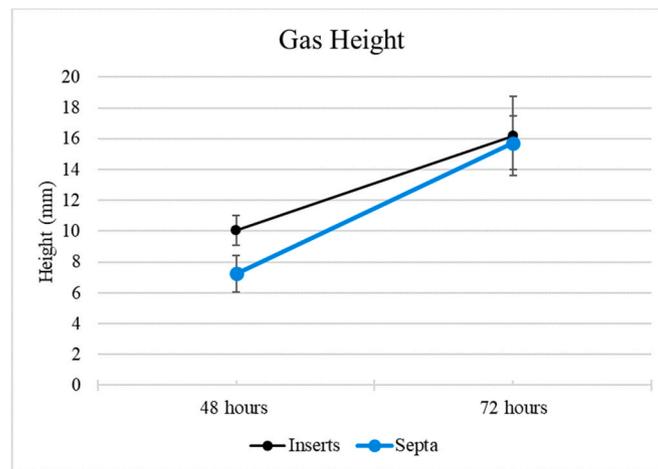
Fig. 14. Displacement of the inserts or septa in the FPAs with the PA14 gas production by incubation time. Error bars represent 95% confidence interval. N = 3 biological replicates.

Appendix D. (Effectiveness of biofilm RNA preservation using a RNAlater: liquid culture ratio of 1:2)

The ThermoFisher Scientific RNAlater user guide suggests pelleting the cells and resuspending them in pure RNAlater solution [30]. Since it was not possible to pellet the biofilm cells before adding the RNAlater, the effectiveness of biofilm RNA preservation when mixed in a 1:2 RNAlater: liquid culture ratio was tested. Five biofilm samples grown over SS316 or LIS were prepared and preserved with this ratio. The dissolved RNAlater was able to preserve the RNA of the biofilm samples and yielded extracted RNA of high integrity (RINe values above 7) and concentration (>1 ng) (see Fig. 15). The presence of clearly defined bands in the TapeStation gel confirms that the RNA was not degraded (see Fig. 15). This confirmed that the protocol would yield enough RNA of good quality to be sequenced for transcriptomics, as minimum input required is 500 pg.
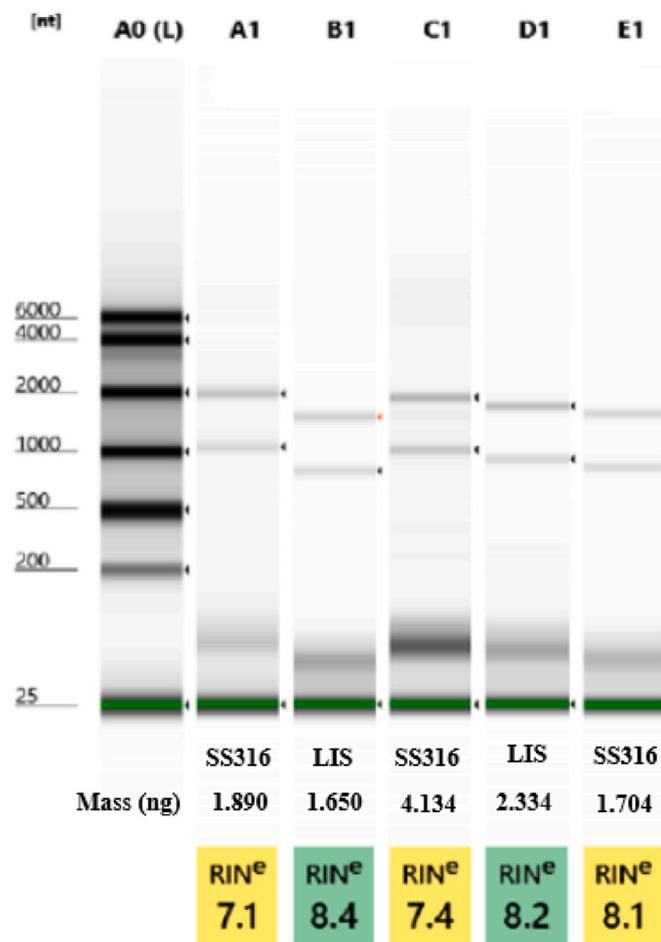

Fig. 15. Biofilm RNA preservation test using a RNAlater: liquid culture ratio of 1:2. TapeStation gel, RNA mass, and RINe values of RNA extracted from biofilms after being preserved with the diluted RNAlater. N = 3 biological replicates for SS316 and 2 replicates for LIS.

Appendix E. (Planktonic cell contamination elimination test)

UspA, the universal stress protein specific to all strains of *E. coli*, is encoded by 434bp in *uspA* gene. The *uspA* primers amplify further up and downstream of the gene giving a total region of 884bp targeted. *UidA* gene encodes for the b-D-glucuronidase enzyme, also unique to *E. coli*. The *uidA* primers amplify a 166bp fragment of the gene and were used to further validate results. In the *uspA* gel (see Fig. 16) and the *uidA* gel (see Fig. 17) only the positive controls: *E. coli* bacterial culture (C+) and *E. coli* planktonic cells collected from the samples (E+), present a band (approx. 884bp for *uspA* and 166bp for *uidA*) as expected. The absence of a band in the negative controls: water (C-) and *P. aeruginosa* bacterial culture (P-), indicate that there was no contamination in the reaction and that the primers are indeed specific for *E. coli*, respectively. The absence of the 884bp (*uspA*) or 166bp (*uidA*) band in the biofilm samples 17–20 double corroborates that the biofilm collection method allows for separation of the biofilm without contamination of planktonic cells.
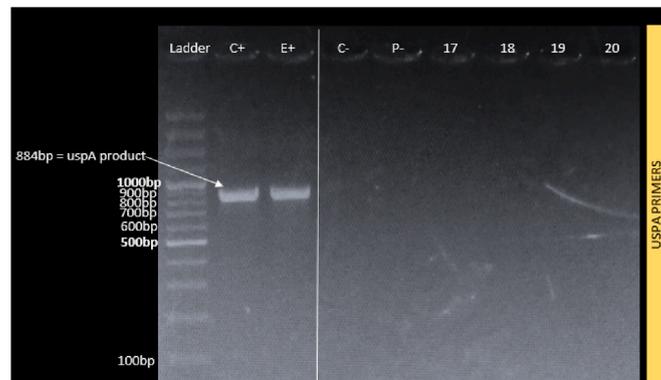

Fig. 16. Electrophoresis gel for biofilm samples 17–20 using primers *uspA*. C+ and E+: positive controls. C- and P-: negative controls.
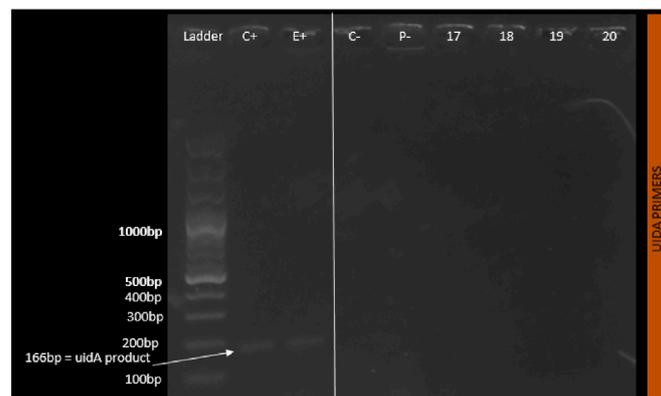

Fig. 17. Electrophoresis gel for biofilm samples 17–20 using primers *uidA*. C+ and E+: positive controls. C− and P−: negative controls.

Appendix F. (Cold stow impact on viability of PA14)

Bacterial inoculum samples were prepared as described in Section 4.2 and then stored at 4 °C. Samples were taken out of cold stow at different times and stained with PI [15 μM] and SYTO 9 [2.5 μM] to differentiate between dead and live cells, respectively. The viability of the inoculum was better at 20 days of cold stow than 1 day of cold stow. Aditionally, 88% (LBK) and 99% (mAUMg-hi Pi) of PA14 cells remained viable at 20 days of cold stow (see Figs. 18 and 19).
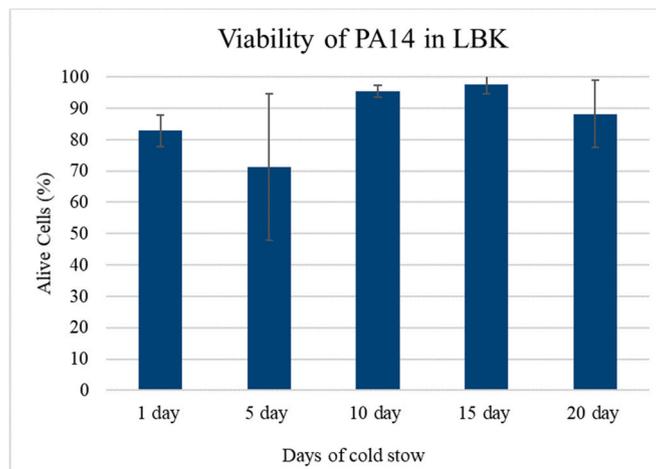
Fig. 18. Viability of *Pseudomonas aeruginosa* PA14 grown in LBK after cold stow at 4 °C. *p-value <0.05. Error bars represent 95% confidence interval. N = 3 biological replicates.
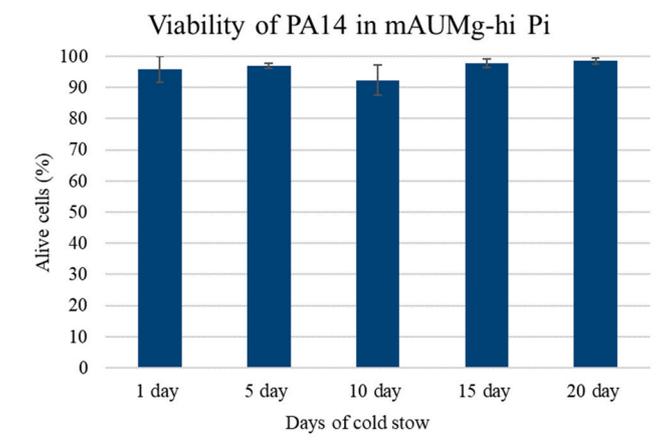

Fig. 19. Viability of *Pseudomonas aeruginosa* PA14 grown in mAUMg-hi Pi after cold stow at 4 °C. *p-value <0.05. Error bars represent 95% confidence interval. N = 3 biological replicates.

Appendix G. (Cold stowed media impact on PA14 growth)

The time that the growth medium was cold stowed before the activation of the experiment, did not impact PA14's ability to growth. There was no significant difference between the cold stowed times up to 6 months (see Fig. 20). Nevertheless, the time that the Space Biofilm experiment had for the pre-ops cold stow was 25 days, far less than the tested 6 months.
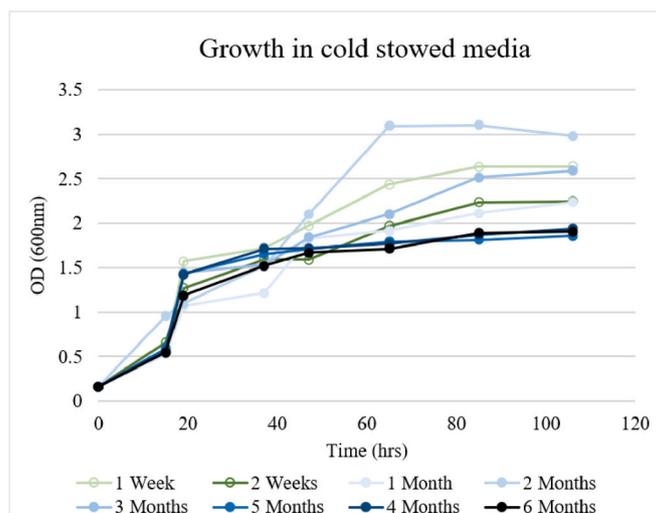

Fig. 20. PA14 growth curves in cold stowed mAUMg-hi Pi medium. N = 1 biological replicate.

Appendix H. (Post-ops cold stow impact on data acquisition)

Samples of one day of incubation were prepared as described in section 4 and processed for either RNA extraction or morphology analysis. The post-ops cold stowage did not affect the RNA quality, nor the microscopy imaging. RNA extracted from samples had good integrity and quantity, enough to perform RNA sequencing (see Table 4). Additionally, z-stacks from biofilm samples were successfully acquired and biofilm mass and thickness were calculated (see Fig. 21).

Table 4
Quality (RIN values) and quantity (mass) results for the RNA extracted from the post-ops cold stow biofilm samples. Color code: white is excellent (RIN ≥5 and mass ≥100 pg), green is good (RIN ≥4 and mass ≥20 pg), yellow is poor (RIN ≥3 and mass ≥10 pg), and red is failure (RIN <3 and mass <10 pg).

Material Coupon	RIN	RNA mass (pg)
SS316	UD*	4296
	UD*	6132
	UD*	20900
tSS316	UD*	16132
	UD*	17384
	UD*	28416
MIT LIS	UD*	71824
	NA*	300
	UD*	6680
Cellulose	8.2	1540
	1.5	80
	UD*	2264
Silicone	6.3	208
	UD*	1092
	2.1	164
Silicone DLIP	9.3	744
	NA*	20
	2.5	372

* NA= not able to determine by software, bad peaks. UD= undetermined because of software malfunction, good peaks.
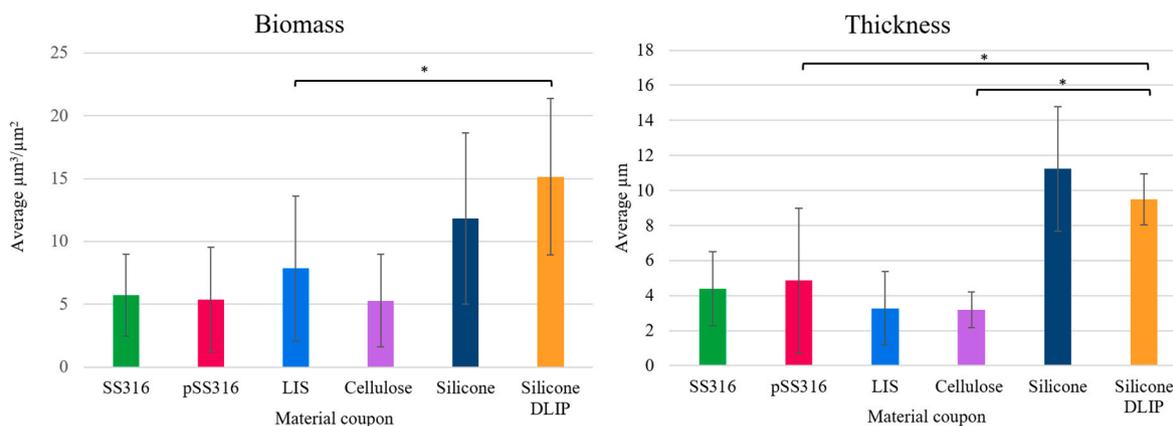

Fig. 21. Biomass and thickness of PA14 biofilms formed over different material surfaces at 1 day of incubation and 64 days of post-ops cold stow. Error bars represent 95% confidence interval. *p-value <0.05. N = 3 biological replicates each imaged in 2 fields of view.

References

[1] S.S. Branda, Å. Vik, L. Friedman, R. Kolter, Biofilms: the matrix revisited, Trends Microbiol. 13 (1) (Jan. 2005) 20–26, https://doi.org/10.1016/j.tim.2004.11.006.

[2] R. Nazir, M.R. Zaffar, I. Amin, Chapter 8 - bacterial biofilms: the remarkable heterogeneous biological communities and nitrogen fixing microorganisms in lakes, in: S.A. Bandh, S. Shafi, N. Shameem (Eds.), Freshwater Microbiology, Academic Press, 2019, pp. 307–340, https://doi.org/10.1016/B978-0-12-817495-1.00008-6.

[3] R. Mansour, A. Elshafei, Role of microorganisms in corrosion induction and prevention, Br. Biotechnol. J. 14 (Jan. 2016) 1–11, https://doi.org/10.9734/BBJ/2016/27049.

[4] P.S. Stewart, J. William Costerton, Antibiotic resistance of bacteria in biofilms, Lancet 358 (9276) (Jul. 2001) 135–138, https://doi.org/10.1016/S0140-6736(01)05321-1.

[5] M. Jamal, et al., Bacterial biofilm and associated infections, J. Chin. Med. Assoc. JCMA 81 (1) (2018) 7–11, https://doi.org/10.1016/j.jcma.2017.07.012.

[6] Ji-Dong Gu, M. Roman, T. Esselman, R. Mitchell, The role of microbial biofilms in deterioration of space station candidate materials, Int. Biodeterior. Biodegrad. 41 (1) (Jan. 1998) 25–33, https://doi.org/10.1016/S0964-8305(98)80005-X.

[7] L. Peterson, Environmental Control and Life Support System (ECLSS)," Presented at the System Engineering Workshop, Ames Research Center, USA, 2009 [Online]. Available: https://ntrs.nasa.gov/archive/nasa/casi.ntrs.nasa.gov/20090029327.pdf. (Accessed 3 December 2019).

[8] L. Zea, et al., Design of a spaceflight biofilm experiment, Acta Astronaut. 148 (Jul. 2018) 294–300, https://doi.org/10.1016/j.actaastro.2018.04.039.

[9] N. Weir, M. Wilson, A. Yoets, T. Molina, R. Bruce, L. Carter, Microbiological characterization of the international space station water processor assembly external filter assembly S/N 01, in: Presented at the 42nd International Conference on Environmental Systems, Jul. 2012, https://doi.org/10.2514/6.2012-3595. San Diego, California.

[10] V. Kak, Infections in confined spaces: cruise ships, military barracks, and college dormitories, Infect. Dis. Clin. 21 (3) (2007) 773–784, https://doi.org/10.1016/j.idc.2007.06.004, ix–x, Sep.

[11] L. Zea, et al., Potential biofilm control strategies for extended spaceflight missions, Biofilms 2 (Dec. 2020) 100026, https://doi.org/10.1016/j.bioflm.2020.100026.

[12] M. Medina, E. Castillo-Pino, An introduction to the epidemiology and burden of urinary tract infections, Ther. Adv. Urol. 11 (May 2019), https://doi.org/10.1177/1756287219832172, 1756287219832172.

[13] J.C. Nickel, J.W. Costerton, R.J.C. McLean, M. Olson, Bacterial biofilms: influence on the pathogenesis, diagnosis and treatment of urinary tract infections, J. Antimicrob. Chemother. 33 (suppl_A) (May 1994) 31–41, https://doi.org/10.1093/jac/33.suppl_A.31.

[14] Mayo Clinic Staff. (n.d.). Urinary tract infection (UTI) - Symptoms and causes. Mayo Clinic. https://www.mayoclinic.org/diseases-conditions/urinary-tract-infection/symptoms-causes/syc-20353447 (accessed Jul. 22, 2022).

[15] J. Law, R. Cole, M. Young, S. Mason, NASA Astronaut Urinary Conditions Associated with Spaceflight," Presented at the 87th Annual Scientific Meeting of the Aerospace Medical Association, Atlantic City, NJ, United States, Apr. 2016 [Online]. Available: https://ntrs.nasa.gov/search.jsp?R=20150020958. (Accessed 2 December 2019).

[16] K. Shigemura, S. Arakawa, Y. Sakai, S. Kinoshita, K. Tanaka, M. Fujisawa, Complicated urinary tract infection caused by Pseudomonas aeruginosa in a single institution (1999–2003), Int. J. Urol. 13 (5) (2006) 538–542, https://doi.org/10.1111/j.1442-2042.2006.01359.x.

[17] G.A. O'Toole, R. Kolter, Flagellar and twitching motility are necessary for Pseudomonas aeruginosa biofilm development, Mol. Microbiol. 30 (2) (Oct. 1998) 295–304, https://doi.org/10.1046/j.1365-2958.1998.01062.x.

[18] S.B. Subramanyam, G. Azimi, K.K. Varanasi, Designing lubricant-impregnated textured surfaces to resist scale formation, Adv. Mater. Interfac. 1 (2) (2014), 1300068, https://doi.org/10.1002/admi.201300068.

[19] W. Kim, et al., Spaceflight promotes biofilm formation by Pseudomonas aeruginosa, PLoS One 8 (4) (Apr. 2013), https://doi.org/10.1371/journal.pone.0062437 e62437.

[20] D.W. Müller, T. Fox, P.G. Grützmacher, S. Suarez, F. Mücklich, Applying ultrashort pulsed direct laser interference patterning for functional surfaces, Sci. Rep. 10 (1) (Feb. 2020) 3647, https://doi.org/10.1038/s41598-020-60592-4.

[21] D.S. Bachoon, F. Chen, R.E. Hodson, RNA recovery and detection of mRNA by RT-PCR from preserved prokaryotic samples, FEMS Microbiol. Lett. 201 (2) (2001) 127–132, https://doi.org/10.1111/j.1574-6968.2001.tb10745.x.

[22] G.E.C. Sheridan, C.I. Masters, J.A. Shallcross, B.M. Mackey, Detection of mRNA by reverse transcription-PCR as an indicator of viability in Escherichia coli cells, Appl. Environ. Microbiol. 64 (4) (Apr. 1998) 1313–1318.

[23] S.M. Hunt, E.M. Werner, B. Huang, M.A. Hamilton, P.S. Stewart, Hypothesis for the role of nutrient starvation in biofilm detachment, Appl. Environ. Microbiol. 70 (12) (Dec. 2004) 7418–7425, https://doi.org/10.1128/AEM.70.12.7418-7425.2004.

[24] J.S. Webb, et al., Cell death in Pseudomonas aeruginosa biofilm development, J. Bacteriol. 185 (15) (Aug. 2003) 4585–4592, https://doi.org/10.1128/JB.185.15.4585-4592.2003.

[25] L.P. Godambe, J. Bandekar, R. Shashidhar, Species specific PCR based detection of Escherichia coli from Indian foods, 3 Biotech 7 (2) (Jun. 2017) 130, https://doi.org/10.1007/s13205-017-0784-8.

[26] J. Chen, M.W. Griffiths, PCR differentiation of Escherichia coli from other gram-negative bacteria using primers derived from the nucleotide sequences flanking the gene encoding the universal stress protein, Lett. Appl. Microbiol. 27 (6) (Dec. 1998) 369–371, https://doi.org/10.1046/j.1472-765x.1998.00445.x.

[27] L. Heijnen, G. Medema, Quantitative detection of E. coli, E. coli O157 and other shiga toxin producing E. coli in water samples using a culture method combined with real-time PCR, J. Water Health 4 (4) (Dec. 2006) 487–498.

[28] Z. Nisar, L. Stodieck, L. Zea, Defining A Spaceflight Biofilm Experiment through Comprehensive Assessment of Material, Media, and Hardware Biocompatibility," Presented at the International Astronautical Congress (IAC), Bremen, Germany, 2018 [Online]. Available: https://iafastro.directory/iac/archive/browse/IAC-18/A2/7/45464/. (Accessed 5 February 2022).

[29] T. Niederwieser, et al., SABL – an EXPRESS Locker-Sized Incubator for Performing Biological Experiments Onboard the ISS, Jul. 2015 [Online]. Available: https://ttu-ir.tdl.org/handle/2346/64364. (Accessed 27 September 2021).

[30] ThermoFisher Scientific. (n.d.). RNAlater™ Stabilization Solution. ThermoFisher. https://www.thermofisher.com/order/catalog/product/AM7020 (accessed Jul. 22, 2022).